

# TiO<sub>2</sub> Nanofoam-Nanotube Array for Surface-Enhanced Raman Scattering

Li Liu<sup>1</sup>, Fan Pan<sup>1</sup>, Chang Liu<sup>1\*</sup>, Liangliang Huang<sup>2\*</sup>, Wei Li<sup>3</sup>, Xiaohua Lu<sup>1</sup>

<sup>1</sup> College of Chemical Engineering, Nanjing Tech University, Nanjing 210009, China

<sup>2</sup> School of Chemical, Biological & Materials Engineering, University of Oklahoma, Norman, 73019, United States

<sup>3</sup> European Bioenergy Research Institute and Aston Institute of Materials Research, Aston University, Birmingham B4 7ET, United Kingdom

*Supporting Information Placeholder*

**ABSTRACT:** By tuning the anodic voltage and the electrochemical reaction time, we have synthesized a series of TiO<sub>2</sub> nanofoam-nanotube array structures via a two-step anodic oxidation process. The produced nanofoam-nanotube array demonstrated a remarkable Raman scattering enhancement. The maximum enhancement factors are  $2.3 \times 10^5$  for methylene blue. Factors such as nanotube pore size, nanofoam and solute concentration have been investigated. The Raman scattering enhancement is attributed to the existence of the nanofoam structure, which enables multiple laser scattering among the periodic voids and allows for the occurrence of Raman scattering. The proposed simple and inexpensive approach can promote the use of TiO<sub>2</sub> materials for SERS applications in chemistry, biology and nanoscience.

Semiconductor-based surface enhanced Raman scattering (SERS) has attracted much attention for its potential application in label-free detecting of biomolecule, trace sensing of chemicals and *in situ* monitoring of chemical reactions<sup>1,2</sup>. Compared with metal-based SERS, which usually use coinage metals (Au, Ag or Cu), semiconductor-based SERS has advantages of low cost and good biocompatibility. On the other hand, semiconductor-based SERS generally has a poor sensitivity: the enhancement factor (EF) is in range of  $10 \sim 10^3$ , inferior to that of coinage metals ( $10^6 \sim 10^{14}$ ). A large number of studies have been carried out to improve EF values of semiconductors, for example, by controlling the band gap, the morphology, the particle size and stoichiometry<sup>3,4</sup>. Titanium dioxide (TiO<sub>2</sub>) is one of the most investigated semiconductors for SERS applications. Zhao et al. investigated SERS performance of TiO<sub>2</sub> substrate since 2008<sup>5-7</sup>, reporting that particle size, surface defects, and morphologies have a significant impact on the enhanced Raman scattering of TiO<sub>2</sub>.

In 2013, Alessandri proposed to use cavities to enhance semiconductor Raman scattering performance<sup>8</sup>. He prepared TiO<sub>2</sub> shell-based spherical resonators by the atomic layer deposition (ALD) method. Those resonators show a remarkable enhancement of Raman scattering. The enhancement is ascribed to the synergistic effects of the high refractive index of shell layer, the multiple light scattering through the spheres, and the geometrical factors. Inspired by this approach, Zhang et al. developed a casting and calcination process to prepare TiO<sub>2</sub> inverse opals, achieving a

good SERS performance,  $EF \sim 10^{4.9}$ . Those progresses have clearly demonstrated that manipulating porous characteristics can improve TiO<sub>2</sub> SERS performance. However, their methods for producing TiO<sub>2</sub> nanopores, such as the ALD and the template synthesis method, are complex and cost expensive. It is of great interest to develop simple, reproducible and scalable methods to produce cavity-based TiO<sub>2</sub> materials for SERS applications.

TiO<sub>2</sub> nanotube arrays can be synthesized by anodic oxidation processes<sup>10</sup>: the length, the pore size and the thickness of TiO<sub>2</sub> nanotube can be easily controlled by the oxidation voltage and the electrochemical reaction time. For example, a two-step anodic oxidation method was recently developed to produce an ultralong ( $\sim 30 \mu\text{m}$ ) TiO<sub>2</sub> nanotube array<sup>11</sup>. With a small voltage, the first anodic oxidation produces the initial TiO<sub>2</sub> nanotube array, which serves as a protective layer for nanotube growth. In general, the protective layer will completely dissolve in the electrolyte solution during the second anodic oxidation.

It is worth pointing out that TiO<sub>2</sub> nanotube array has been adopted as a supporter to gold or silver to improve their SERS performance<sup>12,13</sup>. However, the array itself has not been reported to demonstrate promising SERS performance. In this work, we propose a modified two-step anodic oxidation process to synthesize TiO<sub>2</sub> nanofoam-nanotube array structures. Our produced arrays show excellent enhanced Raman scattering performance for adsorbed Methylene Blue (MB) and cytochrome C.

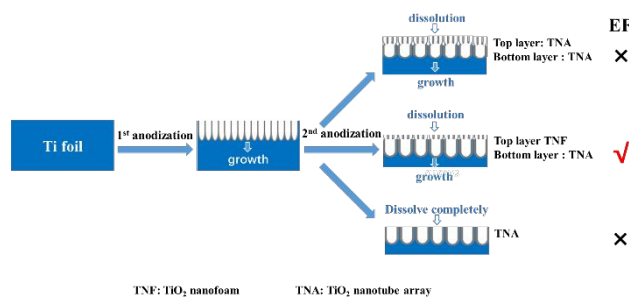


**Figure 1.** A schematic diagram for TiO<sub>2</sub> nanofoam-nanotube array synthesis via a two-step anodic oxidation process.

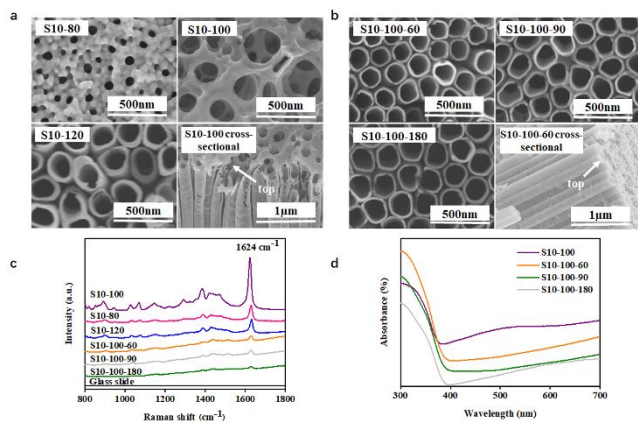


**Figure 2.** Characteristics of synthesized TiO<sub>2</sub> nanotube arrays and their SERS performance. (a) SEM images for samples of group A; (b) SEM images for samples of group B; (c) SERS performance of adsorbed MB ( $10^{-3}$  M); (d) UV-vis absorption spectra.

TiO<sub>2</sub> nanotube arrays with different morphologies were synthesized by the two-step anodic oxidation. A schematic diagram for the synthesis process is shown in Figure 1 and the characterizations are present in Figure 2. In Figure 2, “S10-80” denotes the sample synthesized by: first step, 10 voltage oxidation, for 30 min, which is the default oxidation time unless mentioned otherwise; second step, 80 voltage oxidation, for 30 min. According to this nomenclature, “S10-100-60” is the sample produced by 10 voltage oxidation, for 30 min (step 1), and 100 voltage oxidation, for 60 min (step 2). Two sets of samples have been synthesized and tested, namely, group A: S10-80, S10-100, S10-120; group B: S10-100-60, S10-100-90, S10-100-180. The SEM images of Figure 2(a) and 2(b) reveal that, for group A, the S10-100 sample is composed of two distinguishable parts, the top nanofoam structure (thickness,  $\sim 100$  nm) and the bottom nanotube array (diameter,  $\sim 300$  nm). The nanofoam and nanotube are interconnected, achieving the enhanced Raman scattering, similar to the mechanism of TiO<sub>2</sub> inverse opal structure by Zhang and Co-workers<sup>9</sup>. For a lower 2<sup>nd</sup> oxidation voltage, S10-80, neither the nanofoam nor the nanotube array has fully grown. When the 2<sup>nd</sup> oxidation voltage is increased to 120 V, during the 30 min oxidation, the top nanofoam layer completely dissolves in the electrolyte solution and the nanotube array remain. It is worth emphasizing that the oxidation time is a critical parameter. As shown by group B, by using a same 2<sup>nd</sup> oxidation voltage but a longer oxidation time, that is, from 30 min to 60, 90, and 180 min, respectively, the top nanofoam layer also disappears and none of group B shows a promising SERS performance for Methylene Blue ( $10^{-3}$  M), as illustrated in Figure 2(c). The EF is calculated with respect to the Raman scattering peak at  $1624\text{ cm}^{-1}$ . The EF value for group B is about 1000, which is in accordance with that of TiO<sub>2</sub> nanoparticles. It implies that the slightly enhanced Raman scattering of TiO<sub>2</sub> nanotube array is due to the charge transfer mechanism. On the other hand, the S10-100 sample of TiO<sub>2</sub> nanofoam-nanotube array shows a remarkable SERS performance. The EF is  $2.3 \times 10^5$ , as far as we are aware of, the best reported result for non-plasmon TiO<sub>2</sub> SERS substrate. It is worth noting that the S10-80 sample, without a fully developed TiO<sub>2</sub> nanofoam, shows a poor SERS performance. We report that the existence and the structure of TiO<sub>2</sub> nanofoam significantly affect the SERS performance.

XRD and UV-vis characterizations have been carried out to investigate the Raman enhanced mechanism for these samples. XRD patterns for samples S10-80, S10-100 and S10-120 are shown in Figure S1. All samples consist of anatase crystal phase and titanium metal phase. UV-vis absorption spectra for all samples are

shown in Figure 2 (d), where S10-100 has a better light absorption behavior than others. This further suggests that the enhanced Raman scattering of S10-100 is due to the top nanofoam structure: multiple laser scattering among the periodic voids and more opportunities for the occurrence of Raman scattering.

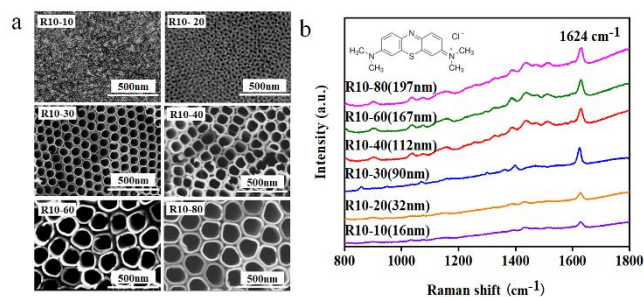


**Figure 3.** The effect of pore size of TiO<sub>2</sub> nanotube single layer on its SERS performance. (a) SEM images of TiO<sub>2</sub> nanotube with different pore size, (b) SERS of  $10^{-3}$  M Methylene Blue adsorbed on TiO<sub>2</sub> nanotube substrates.

**Pore size effect** The aforementioned group A samples have different pore sizes of the nanotube array. In order to understand whether the pore size itself plays a significant role, various TiO<sub>2</sub> nanotube arrays have been synthesized and examined, as illustrated in Figure 3. It is important to note that none of those samples has the nanofoam layer, and that the 1<sup>st</sup> and 2<sup>nd</sup> oxidations are 4 hr and 8 hr, respectively. A longer oxidation time is beneficial to grow longer TiO<sub>2</sub> nanotubes. As shown in Figure 3, when the 2<sup>nd</sup> oxidation voltage increases from 10 V to 80 V, the corresponding TiO<sub>2</sub> pore size goes from 16 nm to 197 nm. But for the broad pore size range, all samples demonstrate regular SERS performance according to the MB Raman peak at  $1624\text{ cm}^{-1}$ . The EF value is around  $5.3 \times 10^3$ . Therefore, the pore size is not the dominating factor for the high EF value ( $2.3 \times 10^5$ ) of the S10-100 sample.

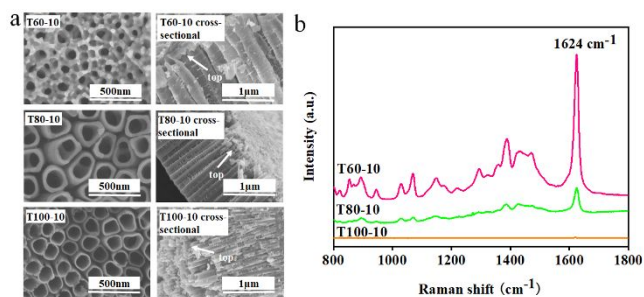


**Figure 4.** The effect of preparation condition on double layer structure and SERS performance of TiO<sub>2</sub> nanotube array. (a) SEM images of different samples, (b) SERS of Methylene Blue ( $10^{-3}$  M) adsorbed on different substrates.

**Nanofoam effect** In order to confirm the critical role of the nanofoam layer for the SERS performance, we modified the oxidization condition, i.e., using a larger voltage for the first oxidation, and a smaller voltage for the second oxidation. A serial of TiO<sub>2</sub> nanotube arrays have been synthesized with or without the nanofoam layer. For the three new samples in Figure 4, only the T60-10 has the nanofoam-nanotube array structure, demonstrating an excellent SERS performance,  $EF \sim 1.0 \times 10^5$ . When the first oxidation voltage increases to 80 V, the produced T80-10 sample no longer has the nanofoam layer, but an ordered TiO<sub>2</sub> nanotube double array. If the first oxidation voltage further increases to 100 V, only ordered single TiO<sub>2</sub> nanotube layer is observed of the T100-10 sample. With this set of samples, we further confirm that the

nanof foam layer is critical for SERS performance, and that the nanof foam-nanotube array is very promising yet easy to synthesize.

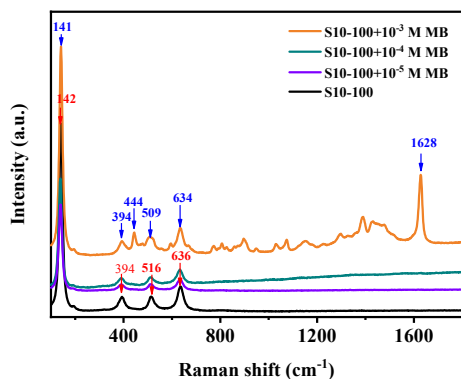


**Figure 5.** SERS of methylene blue with different concentrations on S10-100 sample.

It was reported that probe molecule adsorption on semiconductors can enhance the Raman intensity of phonon modes of the semiconductor substrate, due to interband and charge-transfer resonances<sup>14</sup>. We compare Raman modes of S10-100 sample without and with different MB concentrations. The results are shown in Figure 5. The Raman peaks (142, 394, 516 and 636  $\text{cm}^{-1}$ ) of pristine S10-100 sample are characteristic Raman modes of anatase  $\text{TiO}_2$ . The intensities of those Raman modes are almost unchanged upon MB adsorption, suggesting that the SERS occurred on S10-100 sample is not because of the charge-transfer mechanism. Instead, the enhancement is probably due to the light-matter coupling, similar to what was reported about  $\text{TiO}_2$  photonic microarray by Zhang et al<sup>9</sup>. In addition, Figure 5 reveals that at low MB concentrations,  $10^{-4}$  and  $10^{-5}$  M, there is almost no Raman scattering enhancement at 1628  $\text{cm}^{-1}$ . This is because MB molecules can adsorb on the outer wall or enter the inner space of  $\text{TiO}_2$  nanotube. Therefore, the excellent SERS performance is only observed at reasonably high MB concentrations, such as  $10^{-3}$  M in this work. Future work is needed to improve the sensitivity at low concentrations.

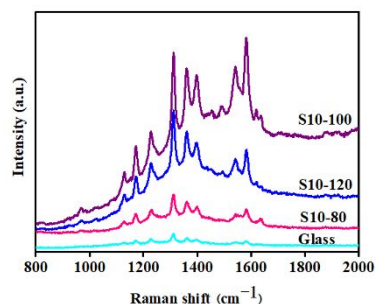


**Figure 6.** SERS of cytochrome c ( $5 \times 10^{-4}$  M) adsorbed on  $\text{TiO}_2$  samples with (S10-100) or without the nanof foam layer (S10-80 and S10-120).

In order to further demonstrate the potential of the  $\text{TiO}_2$  nanof foam-nanotube array, the detection of cytochrome c (Cyt c) has been also tested. As a water-soluble heme protein, Cyt c has been studied for both structural and dynamic properties. Figure 6 shows that the intensities for characteristic modes at 1362  $\text{cm}^{-1}$ , 1496  $\text{cm}^{-1}$ , 1551  $\text{cm}^{-1}$  and 1626  $\text{cm}^{-1}$ , are small on the glass substrate. When Cyt c gets adsorbed on  $\text{TiO}_2$  samples, those Raman modes are enhanced considerably. The best performance is still from the S10-100 sample where a nanof foam-nanotube array structure exists.

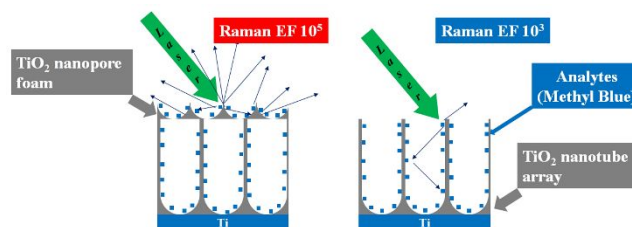


**Figure 7.** The schematic diagram for  $\text{TiO}_2$  nanotube array SERS performance with or without  $\text{TiO}_2$  nanof foam top layer.

In summary,  $\text{TiO}_2$  nanof foam-nanotube array samples have been synthesized by a simple two-step anodic oxidation process. Those samples demonstrate excellent SERS performance for both methylene blue and cytochrome c. For methylene blue, the enhanced factor could reach  $2.3 \times 10^5$ , which is the best reported Raman scattering enhancement so far for  $\text{TiO}_2$  semiconductors. The enhancement is due to the existence of the nanof foam structure, which is similar to the cavity-enhanced Raman scattering mechanism, as illustrated in Figure 7. The simple and inexpensive approach can promote the use of  $\text{TiO}_2$  materials for SERS applications in chemistry, biology and nanoscience.

## ASSOCIATED CONTENT

### Supporting Information

Experimental details, including preparation process, XRD patterns, UV-vis absorption spectra, and the enhancement factor calculation. This material is available free of charge via the Internet at <http://pubs.acs.org>

## AUTHOR INFORMATION

### Corresponding Author

[changliu@njtech.edu.cn](mailto:changliu@njtech.edu.cn); [HLL@ou.edu](mailto:HLL@ou.edu)

### Notes

The authors declare no competing financial interests.

## ACKNOWLEDGMENT

This work was supported by the Natural Science Foundation of China (21878143, 21476106), Joint Research Fund for Overseas Chinese Scholars and Scholars in Hong Kong and Macao Young Scholars (21729601), the fund of State Key Laboratory of Materials-Oriented Chemical Engineering (ZK201702, KL16-01), the Priority Academic Program Development of Jiangsu Higher Education Institutions (PAPD).

## REFERENCES

- (1) Alessandri, I.; Lombardi, J. R., Enhanced Raman Scattering with Dielectrics. *Chem. Rev.* **2016**, 116, 14921-14981.
- (2) Han, X. X.; Ji, W.; Zhao, B.; Ozaki, Y., Semiconductor-enhanced Raman Scattering: Active Nanomaterials and Applications. *Nanoscale* **2017**, 9, 4847-4861.
- (3) Zong, C.; Xu, M. X.; Xu, L. J.; Wei, T.; Ma, X.; Zheng, X. S.; Hu, R.; Ren, B., Surface-Enhanced Raman Spectroscopy for Bioanalysis: Reliability and Challenges. *Chem. Rev.* **2018**, 118, 4946-4980.
- (4) Cong, S.; Yuan, Y. Y.; Chen, Z. G.; Hou, J. Y.; Yang, M.; Su, Y. L.; Zhang, Y. Y.; Li, L.; Li, Q. W.; Geng, F. X.; Zhao, Z. G., Noble Metal-Comparable SERS Enhancement from Semiconducting Metal Oxides by Making Oxygen Vacancies. *Nature Comm.* **2015**, 6, 1-7.
- (5) Yang, L. B.; Jiang, X.; Ruan, W. D.; Zhao, B.; Xu, W. Q.; Lombardi, J. R., Observation of Enhanced Raman Scattering for Molecules Adsorbed on  $\text{TiO}_2$  Nanoparticles: Charge-Transfer Contribution. *J. Phys. Chem. C* **2008**, 112, 20095-20098.

- 1 (6) Jiang, X.; Song, K.; Li, X. L.; Yang, M.; Han, X. X.; Yang, L. B.; Zhao,  
2 B., Double Metal Co-Doping of TiO<sub>2</sub> Nanoparticles for Improvement of  
3 their SERS Activity and Ultrasensitive Detection of Enrofloxacin:  
4 Regulation Strategy of Energy Levels. *Chemistry Select* **2017**, 2, 3099-  
5 3105.
- 6 (7) Yang, L. B.; Gong, M. D.; Jiang, X.; Yin, D.; Qin, X. Y.; Zhao, B.;  
7 Ruan, W. D., Investigation on SERS of Different Phase Structure TiO<sub>2</sub>  
8 Nanoparticles. *J. Raman Spectra*. **2015**, 46, 287-292.
- 9 (8) Alessandri, I., Enhancing Raman Scattering without Plasmons:  
10 Unprecedented Sensitivity Achieved by TiO<sub>2</sub> Shell-Based Resonators. *J.*  
11 *Am. Chem. Soc.* **2013**, 135, 5541-5544.
- 12 (9) Qi, D. Y.; Lu, L. J.; Wang, L. Z.; Zhang, J. L., Improved SERS  
13 Sensitivity on Plasmon-Free TiO<sub>2</sub> Photonic Microarray by Enhancing  
14 Light-Matter Coupling. *J. Am. Chem. Soc.* **2014**, 136, 9886-9889.
- 15 (10) Lee, K.; Mazare, A.; Schmuki, P., One-Dimensional Titanium Dioxide  
16 Nanomaterials: *Nanotubes*. *Chem. Rev.* **2014**, 114, 9385-9454.
- 17 (11) Wang, X. Y.; Sun, L. D.; Zhang, S.; Wang, X., Ultralong, Small-  
18 Diameter TiO<sub>2</sub> Nanotubes Achieved by an Optimized Two-Step  
19 Anodization for Efficient Dye-Sensitized Solar Cells. *ACS Appl. Mater. &*  
20 *Infer.* **2014**, 6, 1361-1365.
- 21 (12) Ling, Y. H.; Zhuo, Y. Q.; Huang, L.; Mao, D. L., Using Ag-embedded  
22 TiO<sub>2</sub> Nanotubes Array as Recyclable SERS Substrate. *Appl. Surf. Sci.* **2016**,  
23 388, 169-173.
- 24 (13) Li, X. H.; Chen, G. Y.; Yang, L. B.; Jin, Z.; Liu, J. H., Multifunctional  
25 Au-Coated TiO<sub>2</sub> Nanotube Arrays as Recyclable SERS Substrates for  
26 Multifold Organic Pollutants Detection. *Adv. Func. Mater.* **2010**, 20, 2815-  
27 2824.
- 28 (14) Ma, S.; Livingstone, R.; Zhao, B.; Lombardi, J. R., Enhanced Raman  
29 Spectroscopy of Nanostructured Semiconductor Phonon Modes. *J. Phys.*  
30 *Chem. Lett.* **2011**, 2, 671-674.
- 31  
32  
33  
34  
35  
36  
37  
38  
39  
40  
41  
42  
43  
44  
45  
46  
47  
48  
49  
50  
51  
52  
53  
54  
55  
56  
57  
58  
59  
60